6.2 ANALYSIS OF COLD POOL FORMATION AND EROSION IN THE OWENS VALLEY REGION OF CALIFORNIA

Adam J. Christman[1,*], Ronald Calhoun[1], Andreas Wieser[2], H.J.S. Fernando[1]

[1]Arizona State University, Tempe, Arizona

[2]Forschungszentrum Karlsruhe, Karlsruhe, Germany

1. INTRODUCTION

Atmospheric boundary-layer evolution has been the subject of numerous studies. It was again the focus of the Terrain-Induced Rotor Experiment (T-REX), held in Independence, California in the Owens Valley region during March and April of 2006. Owens Valley lies between the Sierra Nevada mountain range to the west and the White/Inyo mountain range to the east. The highest peak in the contiguous United States of Mt. Whitney, measuring 4,421 m ASL, is located in the Sierra range. The adjacent valley floor lies at approximately 1,200 m ASL, which is bordered by the Inyo mountain range with a peak of 3,390 m ASL making the decent into the valley one of the steepest in the world and creating a quasi-two-dimensional terrain. This was also the motivating factor for intensive study of the region. As such, the primary focus of T-REX was to further investigate the flow of air masses over this complex terrain. Specifically, the goal was to utilize the extensive amount of in-situ instrumentation to observe the interaction of (primarily) westward flowing upper air masses over the Sierra Nevada's as they relate to the formation of standing waves and the at-times accompanying rotor activity.

As a supplement to the investigation of wave activity over the Sierra's, periods of relative quiescent conditions were studied during Extensive Operation Periods (EOPs). The aim of the EOPs was to gather insight into boundary-layer structure and evolution in the absence of large scale phenomena. During these quiescent periods, it is hoped that the diurnal boundary layer cycles can be clearly observed since thermal forcing can be expected to have a significant impact on NBLs (Grubisic, 2004). Most importantly, it is hoped that the formation and erosion of cold pool inversion layers can be clearly observed in such a deep valley. It has been shown for a variety of valleys and basins that the primary source of cold pool erosion is from thermal forcing (Whiteman et. al., 2004; Clements, et. al., 2003) and that along-valley air flow has a negligible effect on the breakup of cold pools (Whiteman et. al., 2004).

Presented here is a study using instruments from Arizona State University to observe under what conditions cold pools will form in the Owens Valley and how the morning onset of thermal forcing compares to turbulent shear from upper-level air flow in the contribution to destruction of cold pools.

2. INSTRUMENTATION

ASU brought numerous instruments to the experimental site in Independence, CA. Among them were a WindTracer Doppler Lidar (from Coherent Technologies), a Scintec sodar/RASS profiler, and a 12m instrumented energy budget tower comprised of 1) Two RM Young sonic anemometers 2) a Campbell Scientific ultra-sonic anemometer 3) temperature/RH probe 4) Kipp & Zonen net radiometer 5) fine-wire thermocouple 6) krypton hygrometer 7) barometric pressure gauge 8) soil heat flux plate and 9) four soil temperature probes. Figure 1 shows the layout of the instruments along the valley floor, just south and east of the town of Independence. The GPS coordinates of the Lidar, sodar, and tower are 36.79753N/118.17578W, 36.787983N/118.178417W, and 36.79827N/118.17478W, respectively.

Lidar scans were used to detect wind fields at the crests of the Sierra Nevada range in an attempt to determine whether the dominant overhead airflow over the mountains was able to penetrate the valley and thus disrupt the

* *Corresponding author address:* Adam J. Christman, Arizona State University, Dept. of Mechanical and Aerospace Engineering, Tempe, AZ 85287; e-mail: adam.christman@asu.edu

nocturnal boundary layer. The sodar/RASS was able to provide vertical temperature profiles and wind velocity fields to determine the presence or absence of the inversion layer and to follow the progression of its formation and destruction. The profiles' ranges were from about 75 m to 600 m with the Lidar giving data up to the 4 km mark at the peaks of the Sierras. The tower data was able to fill the lower gap up to 12 m with the anemometers placed at 1.9 m, 7.3 m, and 11.4 m heights.

With instruments able to give feedback at nearly all levels of the lower atmospheric boundary layers, it is hoped that a significantly complete

2.1 *Observational Periods*

Over the duration of T-REX there were five designated EOP periods, 1 through 5, during which conditions were well suited for the formation of cold pools. Table 1 shows the dates and times of these EOPs. ASU's Lidar was running both RHI and PPI scans continuously during EOPs 2-5 and the sodar/RASS unit was running continuously as well, using 30-minute averages during EOPs 1, 2, and 4 and using 20-minute averages during EOP 3. The system did not log data during EOP 5. The tower ran continuously throughout the campaign, taking 1 Hz data from the soil temperature probes and the soil heat flux plate while taking 10 Hz data from the remaining instruments.

As a result of missing data during portions of EOP 1 and EOP 5, only EOPs 2-4, with complete data sets, are presented here for detailed analysis. Though each EOP lasted 21 hours, the focus will remain on the hours from approximately 05:00 UTC until 18:00 UTC of the second day of each EOP, as this is the period during which the NBL initially forms its most distinctive features and continues on to its dissipated state. As the NBL structure is a strong function of incoming solar insolation, listed in Table 1 are also the astronomical twilight hours for each EOP.

3. RESULTS

The nocturnal boundary layer with its associated cold pool was successfully visualized in each of EOPs 2, 3, and 4. Conditions supported the NBL formation, as winds were extremely light to calm from 07:00 to 18:00 UTCthe night of 30 March at heights from 75 m to 400 m as seen in Figure 2. Figure 3 shows the vertical temperature profile at the start of the cold pool formation. Its onset occurs at about 07:00 UTC or slightly earlier from approximately 100m to 250m in height and continues to grow until it reaches its maximum size of about 2.5K with a height from 190 m to 275 m at 14:00 UTC. With sunrise at 12:24 UTC (Table 1) there will be a delay before sunlight breaches the eastern mountain range to begin the thermal heating of the valley floor. If we take this interval to be approximately 1hr 36min as displayed in Figure 4, to the start of cold pool erosion, it can be compared to the other EOPs on a similar temporal scale. By 16:30 UTC (Figure 4) the inversion had completely receded, taking a total of about 2.5h. Also notable in Figure 4 is the significant change in boundary layer form over the short span from 16:00 UTC to 16:30 UTC, after which it has nearly completely dissipated.

The wind velocity profile for EOP 3 significantly differs from that of EOP 2. Figure 5 shows that it is, in fact, nearly inverted conditions, as winds are mildly sustained from the north at about 6 m/s at elevations from 50m to 200m and from the northwest below 50m and above 200m to 600m at about 12 m/s during the time of inversion and become calm as the sun rises and the inversion layer dissipates. Despite the added turbulence, the inversion layer does indeed form with a maximum size of about 2.5K at 14:40 UTC from 100m to 200m, as shown in the close-up Figure 7. Figure 7 also shows that the inversion break-up occurs in only about 1h time, as it still exists at 14:40 UTC (at its maximum) but is no longer present at 15:40 UTC.

EOP 4 is similar to EOP 3 with prevailing northwesterly winds at roughly 8-10 m/s, slowly dying off with both increasing time and increasing height (Figure 8). Early stages of inversion formation (in Figure 9) appear to show its base at roughly 200m stretching to the end of data input. As the inversion approaches its maximum size, it appears to sink somewhat close to ground level to about 75m before reaching maximum inversion of 3K at 15:00 UTC from 190m to 375m. The height of this inversion is considerably higher than either of the other two under consideration. Once again there is also a fast response dissipation rate. The inversion is destroyed in about 1h from its maximum at 15:00 UTC to 16:00 UTC.

4. DISCUSSION

Many of the results found in the T-REX campaign concerning cold pool formation and destruction are in accord with previous studies. The depth of the Owens Valley was in our favour in determining any relative importance to dominant overhead air flow to cold pool erosion. This hypothesis has been countered in the past during valley and sinkhole studies performed by Whiteman, et. al. (2004). It was shown that cold pool formation and NBLs form in similar manners in both valleys and sinkholes. Not only did this show that upper level disturbances (air flow above sinkholes) did not affect the NBL, but also that along-valley flows played a minimal role at most in distortion or destruction of NBLs. As a result of this, since the Owens Valley is a quasi-two-dimensional valley with the top of the NBL lying below both ridgelines (a maximum observed height of 375m), we can arrive at two conclusions. 1) Any dominant eastward air flow over the Sierra Nevada mountain range is extremely unlikely to contribute to cold pool erosion and 2) Any differences in NBL morphology between distinct times within the valley is unlikely due to differences in dominant valley flow.

At this time Lidar data is not yet available to further investigate these upper level air disturbances. However, once incorporated in the study, these data should prove telling as to the precise interaction of the upper level air flows over the Sierra Nevada's with the air flows within the valley. Nevertheless, the sodar/RASS was able to return data from above the NBL, showing slight to moderate shear at the NBL as seen in Figures 7 and 8. Both EOP 3 and 4 saw more shear than EOP 2, yet no striking differences exist between EOPs 3 and 4 and EOP 2. It can be said that EOP 3 and EOP 4 have temperature profiles restricted to a smaller overall delta-T than EOP 2, but this may be the result of seasonal changes.

There is also a clear progression for the NBL to dissipate faster as the spring season enters its later stages. Not only does it take less time to dissipate, but it forms its maximum inversion later in the day and also becomes fully dissipated later in the day, despite an earlier sunrise and hence an earlier onset of solar insolation, as seen in Figures 11 a), b), and c).

5. CONCLUSION

It is clear that the data collected during T-REX is very much along the lines of previously studied cold pool events. While this is a fair first step towards elucidating these events in the Owens Valley, there is certainly more to be seen as the Lidar data becomes available and incorporated. Furthermore, energetic analysis and computations for sensible heat flux may prove quite telling, since some simplifications may be made concerning the extremely low relative humidity in the valley, along with the valley's homogeneous vegetation and sandy soils.

REFERENCES

Clements, C. B., Whiteman, C. D., and Horel, J. D., 2003: Cold-air-pool structure and evolution in a mountain basin: peter sinks, utah. *J. Appl. Meteor.*, **42**. 752-768.

Grubisic, V., et. al., 2004: T-REX terrain-induced rotor experiment overview document and experiment design.

Whiteman, C. D. et. al., 2004: Inversion breakup in small rocky mountain and alpine basins. *J. Appl. Meteor.*, **43**. 1069-1082.

Figure 1: Locations of Arizona State University's T-REX Instrumentation. All three locations are oriented in the center of the valley between the mountain ranges.

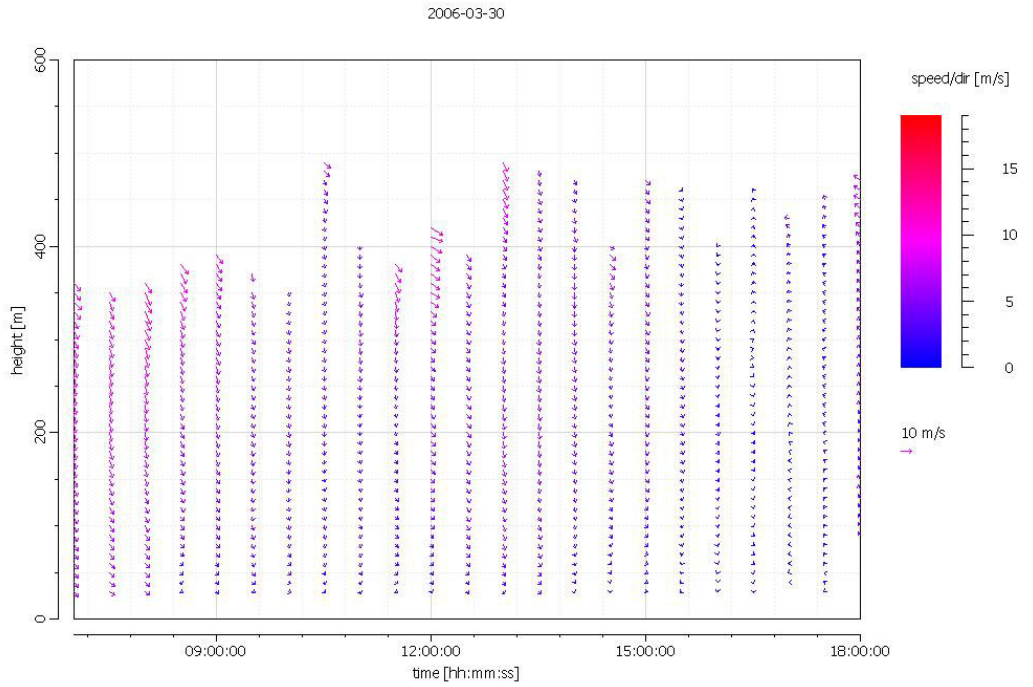

Figure 2: Wind velocity field for EOP 2 during the formation and destruction of a cold pool event (07:00-18:00 UTC) as reported by sodar/RASS using 30-minute averages.

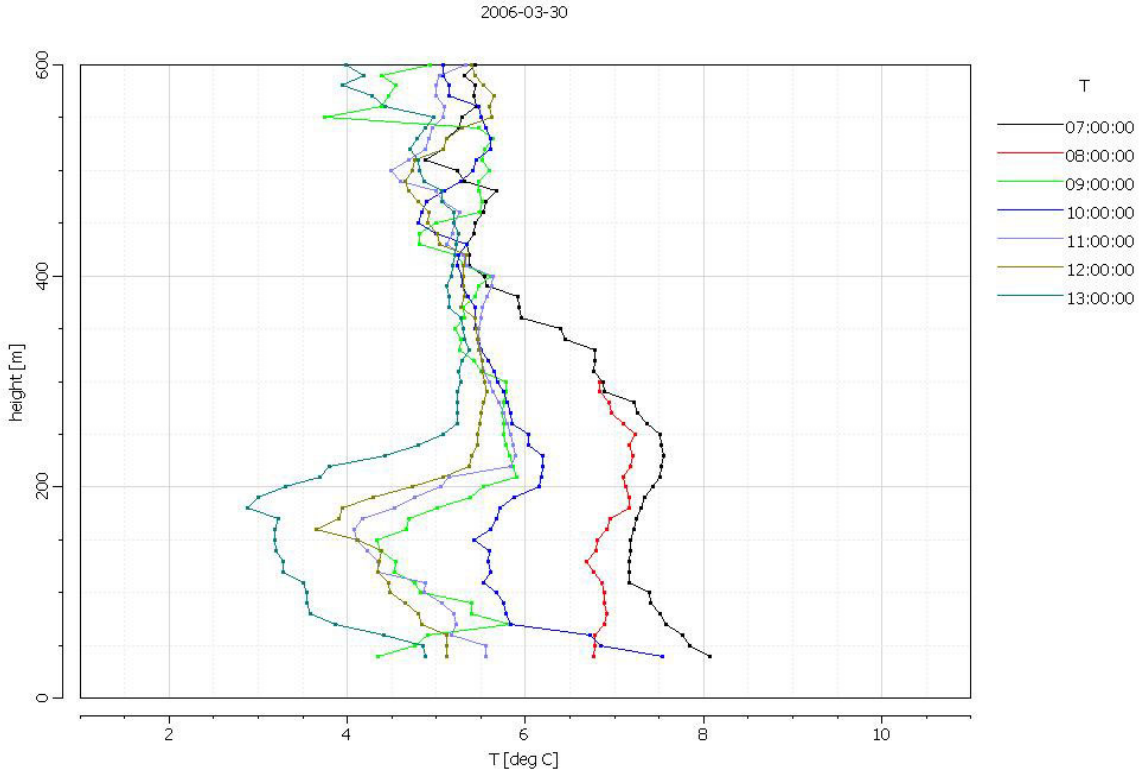

Figure 3: Vertical temperature profile reported from sodar/RASS at hourly intervals from 07:00-13:00 UTC of EOP 2.

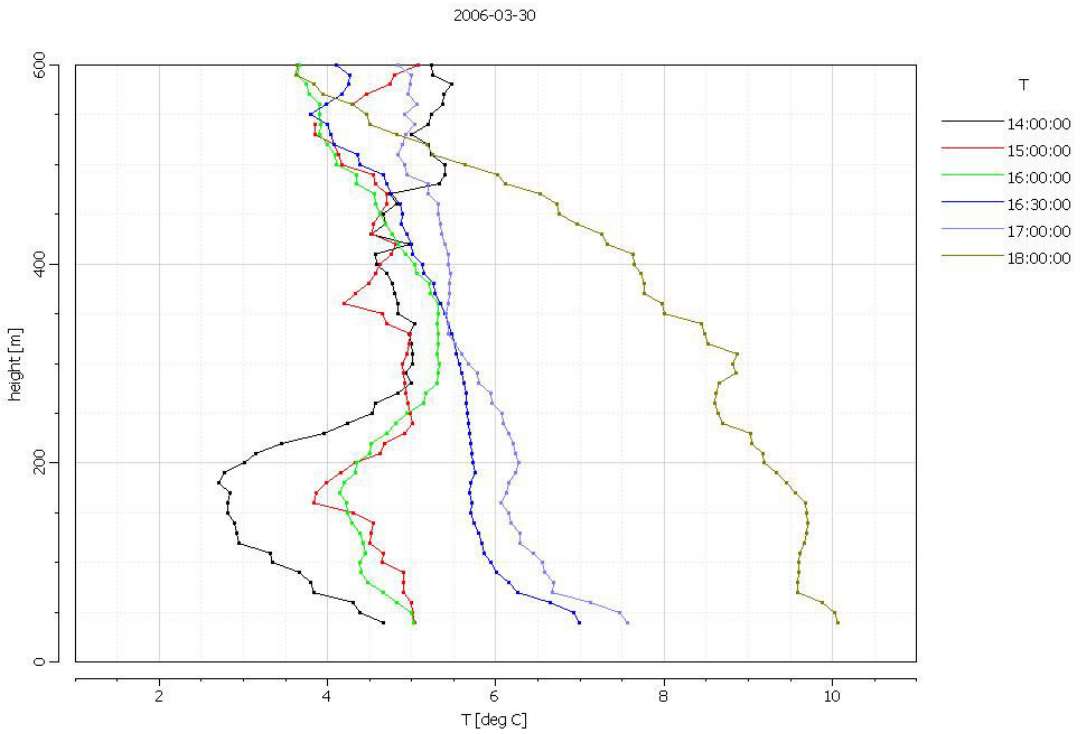

Figure 4: Vertical temperature profile reported from sodar/RASS at hourly intervals from 14:00-18:00 UTC of EOP 2.

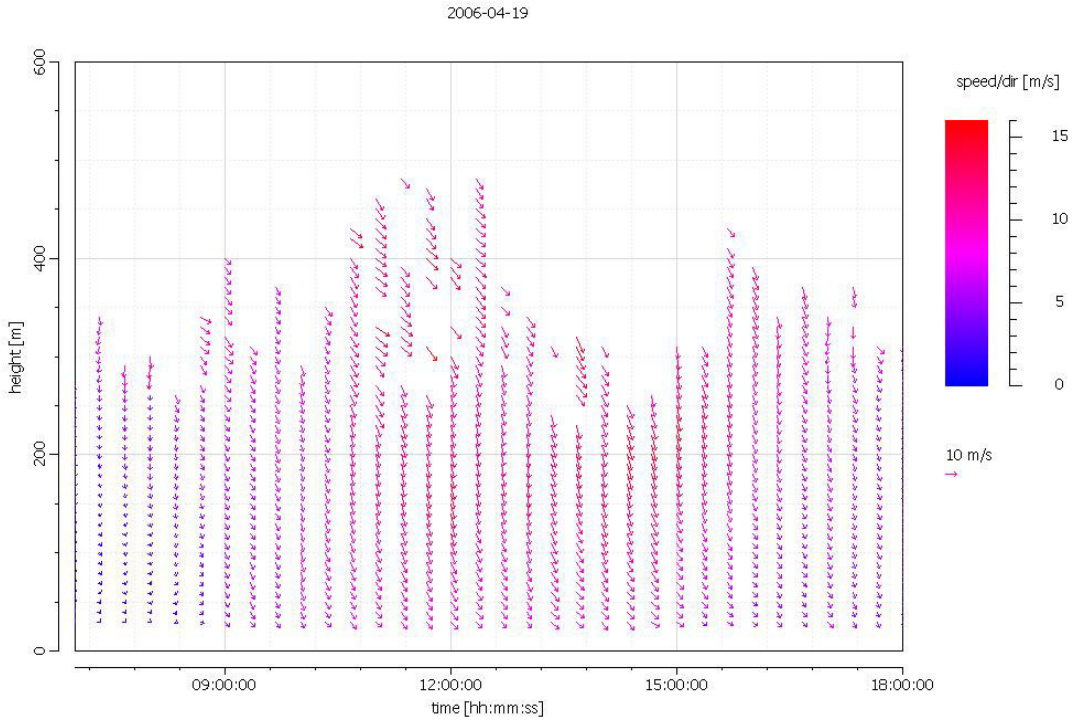

Figure 5: Wind velocity field for EOP 3 during the formation and destruction of a cold pool event (07:00-18:00 UTC).

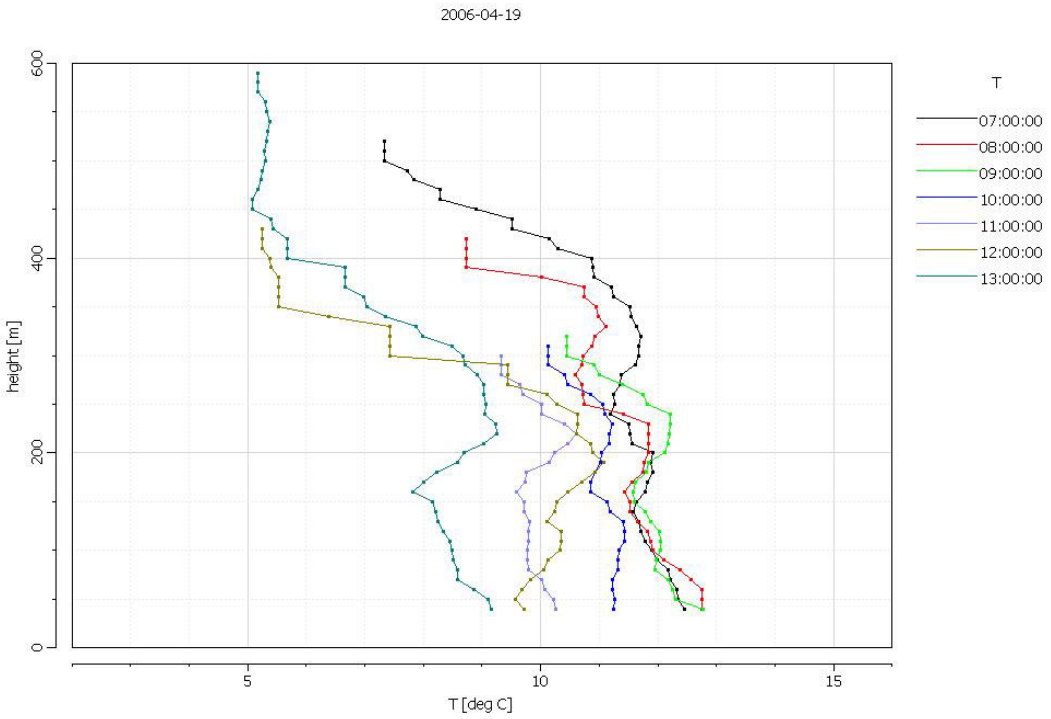

Figure 6: Vertical temperature profile reported from sodar/RASS at hourly intervals from 07:00-13:00 UTCof EOP 3.

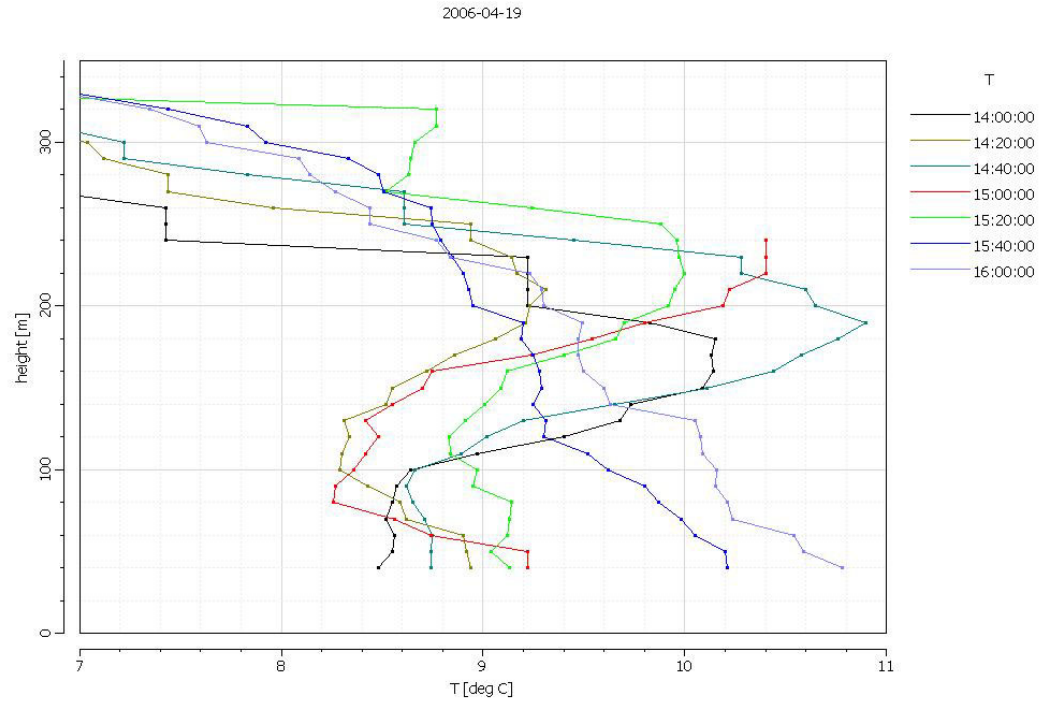

Figure 7: A close-up vertical temperature profile reported from sodar/RASS at 20-minute intervals from 14:00-16:00 UTC of EOP 3.

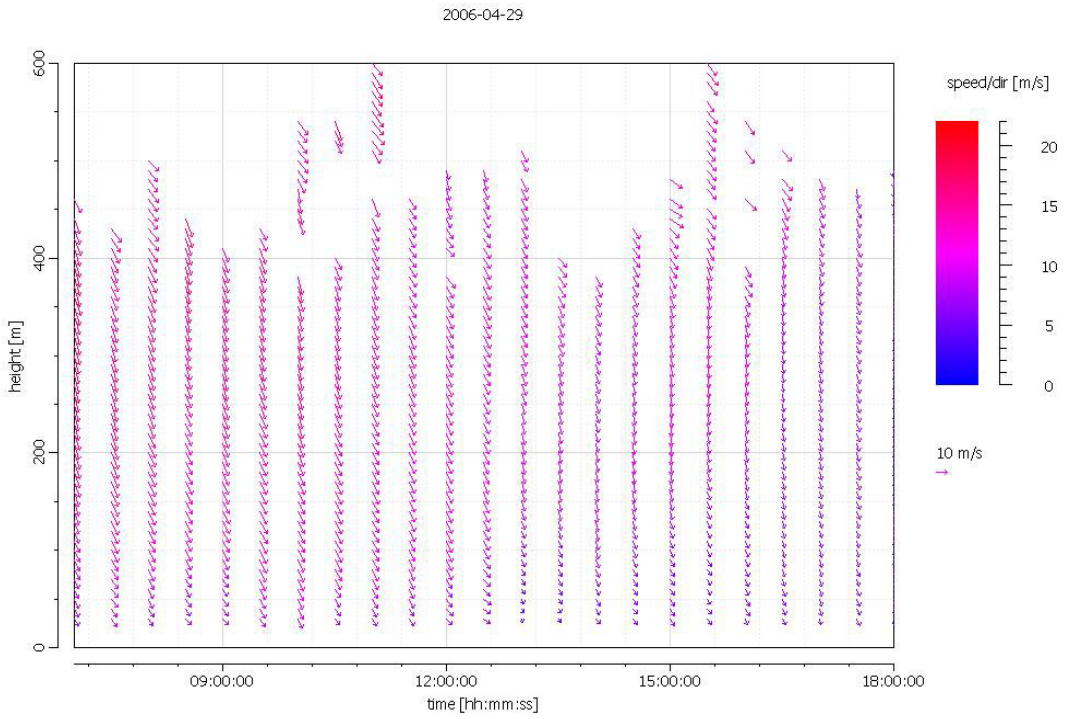

Figure 8: Wind velocity field for EOP 4 during the formation and destruction of a cold pool event (07:00-18:00 UTC).

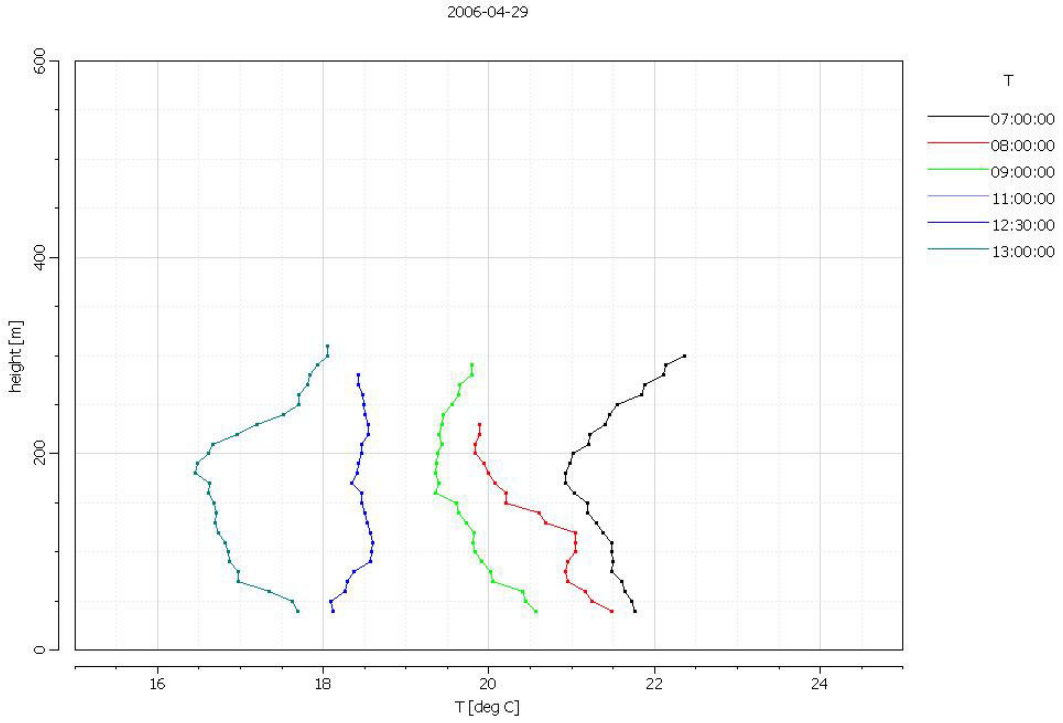

Figure 9: Vertical temperature profile reported from sodar/RASS at hourly intervals from 07:00-13:00 UTC of EOP 4.

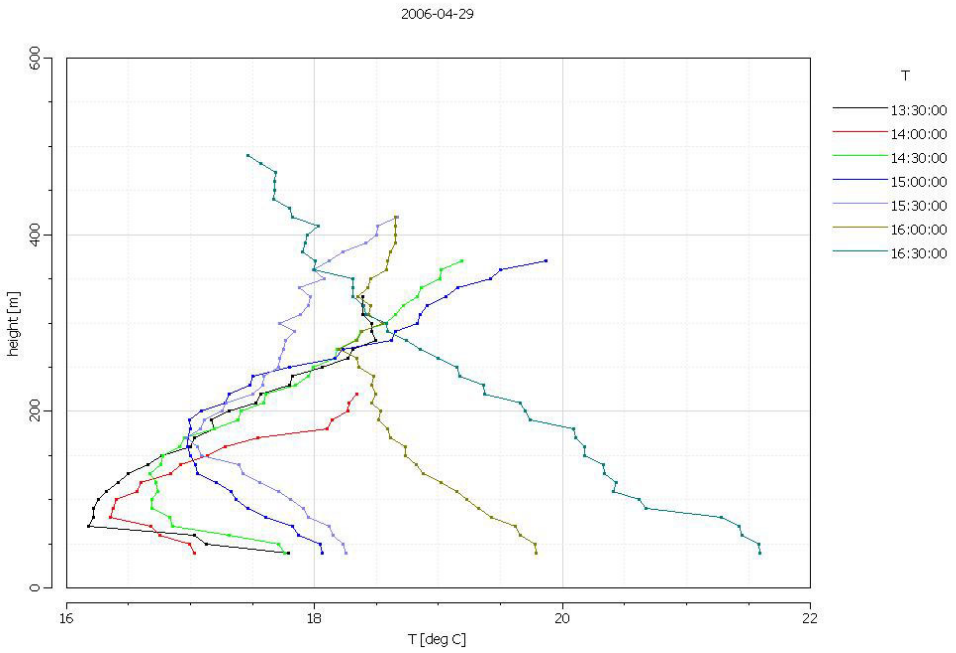

Figure 10: Vertical temperature profile as reported from sodar/RASS at 30-minute intervals from 13:30-16:00 UTC of EOP 4.

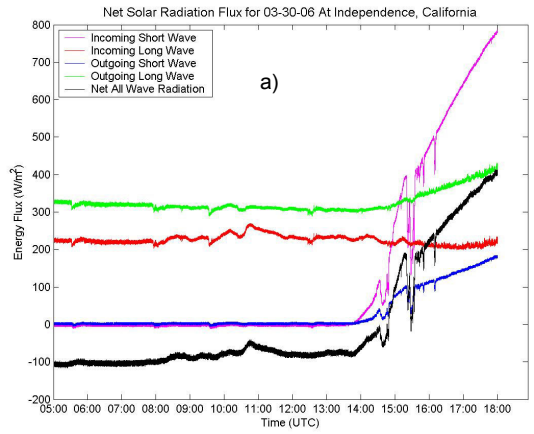

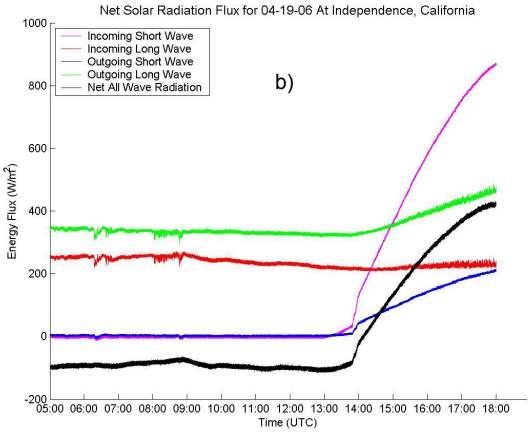

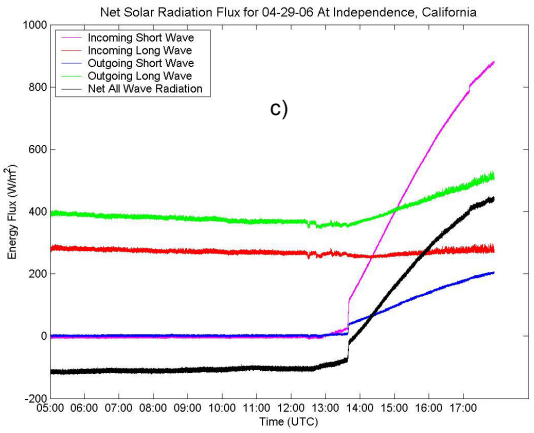

Figure 11a, b, c: Calculations of net incoming solar radiation for (a) EOP 2, (b) EOP 3, and (c) EOP 4. Net radiation is shown in black.

EOP No.	Start Date/Time (DD/MM/YY)/(UTC)	End Date/Time (DD/MM/YY)/(UTC)	Astronomical Twilight Set (UTC)	Astronomical Twilight Rise (UTC)
1	22/03/06 23:00	23/03/06 20:00	03:35	12:24
2	29/03/06 23:00	30/03/06 20:00	03:43	12:13
3	18/04/06 23:00	19/04/06 20:00	04:06	11:39
4	28/04/06 23:00	29/04/06 20:00	04:18	11:23
5	29/04/06 23:00	30/04/06 20:00	04:20	11:22

Table 1: EOP number and its corresponding start and end date/time, with accompanying Twilight rise and set times.